

Extension of the Active-Orbital-Based and Adaptive CC($P;Q$) Approaches to Excited Electronic States: Application to Potential Cuts of Water

Karthik Gururangan^a, Jun Shen^a, Piotr Piecuch^{a,b,*}

^aDepartment of Chemistry, Michigan State University, East Lansing, Michigan 48824, USA

^bDepartment of Physics and Astronomy, Michigan State University, East Lansing, Michigan 48824, USA

Abstract

We report the first study using active-orbital-based and adaptive CC($P;Q$) approaches to describe excited electronic states. These CC($P;Q$) methodologies are applied, alongside their completely renormalized (CR) coupled-cluster (CC) and equation-of-motion (EOM) CC counterparts, to recover the ground- and excited-state potential cuts of the water molecule along the O–H bond-breaking coordinate obtained in the parent CC/EOMCC calculations with a full treatment of singles, doubles, and triples (CCSDT/EOMCCSDT). We demonstrate that the active-orbital-based and adaptive CC($P;Q$) approaches closely approximate the CCSDT/EOMCCSDT data using significantly reduced computational costs while improving the CR-CC and CR-EOMCC energetics in stretched regions of the O–H bond-breaking potentials.

Keywords: Coupled-Cluster Theory, Equation-of-Motion Coupled-Cluster Formalism, Completely Renormalized Coupled-Cluster Approaches, Active-Space Coupled-Cluster Methods, Active-orbital-based CC($P;Q$) Approaches, Adaptive CC($P;Q$) Methodology, Ground- and Excited-State Potential Surfaces of Water

1. Introduction

The development of accurate and computationally practical methods for describing excited electronic states and potential energy surfaces (PESs) of molecules is a vital component of quantum chemistry. This task becomes especially challenging when examining excited states dominated by two- or other many-electron transitions and larger regions of excited-state PESs, which are relevant to spectroscopic and photochemical applications. It is nowadays well established that the excited-state extensions of the coupled-cluster (CC) theory [1–3] belonging to the equation-of-motion (EOM) [4, 5], linear-response (LR) [6–9], and symmetry-adapted-cluster configuration interaction (CI) [10] hierarchies are capable of providing reliable and systematically improvable description of excited electronic states using polynomial computational steps within a conceptually straightforward single-reference (SR) ansatz.

In the EOMCC framework, which is a focus of the present study, the exact excited states of the N -electron system are defined as $|\Psi_\mu\rangle = R_\mu|\Psi_0\rangle$, where $|\Psi_0\rangle = e^T|\Phi\rangle$ is the ground-state CC wave function, with $|\Phi\rangle$ designating the reference determinant that serves as a Fermi vacuum, and $T = \sum_{n=1}^N T_n$ and $R_\mu = \sum_{n=0}^N R_{\mu,n} = r_{\mu,0}\mathbf{1} + \sum_{n=1}^N R_{\mu,n}$ ($\mu > 0$) are the cluster and EOM excitation operators, with T_n and $R_{\mu,n}$ representing their n -body components ($\mathbf{1}$ is the identity operator). The EOMCC approximations obtained by truncating T and R_μ at a given many-body rank provide a transparent route for computing increasingly accurate and systematically improvable excited-state energetics and properties, but the leading and most practical EOMCC approach with singles and doubles (EOMCCSD) [5], obtained by truncating T and R_μ at their two-body components, cannot handle multireference (MR) correlation effects characterizing excited states dominated by two or other many-electron transitions and excited-state potentials outside the Franck–Condon region, especially when chemical bonds are significantly stretched or broken [11–13]. In fact, EOMCCSD is not fully quantitative in describing singly excited states either [14]. In general, higher-level EOMCC

*Corresponding author

Email address: piecuch@chemistry.msu.edu (Piotr Piecuch)

methodologies that incorporate T_n and $R_{\mu,n}$ components with $n > 2$, such as the EOMCC approach with a full treatment of singles, doubles, and triples (EOMCCSDT) [11, 12, 15], in which T and R_μ are truncated at T_3 and $R_{\mu,3}$, respectively, are necessary to obtain an accurate and more robust description.

Inspired by Refs. [13, 16], in this work we focus on converging the ground- and excited-state PESs of the water molecule along the O–H bond-breaking coordinate corresponding to the $\text{H}_2\text{O} \rightarrow \text{H} + \text{OH}$ dissociation obtained with EOMCCSDT and its ground-state CCSDT counterpart [17, 18]. As shown in this study, the CCSDT/EOMCCSDT water potentials are nearly exact, closely matching the full CI data reported in Refs. [13, 16], but the application of the full CCSDT and EOMCCSDT methods, especially when larger molecules and basis sets are considered, is hindered by the expensive computational steps that scale as \mathcal{N}^8 with system size \mathcal{N} . To address this concern, a variety of approximate EOMCC and LRCC schemes aimed at reducing the prohibitive computational costs of the EOMCCSDT and LRCCSDT calculations have been developed. Among them are methods that rely on perturbative arguments to correct the EOMCCSD or LRCCSD calculations for T_3 and $R_{\mu,3}$ effects in an iterative or noniterative fashion [19–22], but these kinds of approaches, while accurate for excited states dominated by one-electron transitions, struggle when the more MR excited states dominated by two-electron transitions are examined. The newer triples corrections to EOMCCSD [13, 14, 23–28], such as the left-eigenstate completely renormalized (CR) EOMCC approach abbreviated as CR-EOMCC(2,3) [26, 27, 29] and its rigorously size-intensive δ -CR-EOMCC(2,3) modification [14, 28] that rely on the moment energy expansions [25–27, 29–34], are more robust in this regard [13, 14, 35], but they may still encounter difficulties when T_3 and $R_{\mu,3}$ correlations become larger, nonperturbative, and strongly coupled to their lower-rank T_1 , T_2 , $R_{\mu,1}$, and $R_{\mu,2}$ counterparts [29, 36, 37]. This becomes evident when examining stretched regions of certain excited-state water potentials with CR-EOMCC(2,3) [13] (cf. Sec. 3.3).

A robust solution to the above deficiencies of the perturbative corrections to EOMCCSD and their CR-EOMCC(2,3) and similar counterparts is offered by the $\text{CC}(P;Q)$ framework [29, 36–40], which generalizes the original CR-CC [26, 30, 31, 33, 34, 41] and CR-EOMCC [14, 25–28] approaches to unconventional truncations in the T and R_μ operators that incorporate the leading contributions to the T_n and $R_{\mu,n}$ components with $n > 2$ into the iterative parts of the computations, correcting the resulting energies for the missing correlation effects of interest using moment expansions similar to those used in CR-CC/EOMCC. In particular, the $\text{CC}(P;Q)$ formalism provides a flexible and powerful framework for converging high-level CC/EOMCC energetics, such as CCSDT, CCSDTQ [42, 43], EOM-CCSDT, etc., at small fractions of the computational costs. The existing $\text{CC}(P;Q)$ methods aimed at recovering the CCSDT and EOMCCSDT energetics include the active-orbital-based $\text{CC}(t;3)$ approach [29, 36], which corrects the CCSDt [44–47] and EOMCCSDt [11, 12, 47] calculations for those T_3 and $R_{\mu,3}$ correlations that are missing in CCSDt/EOMCCSDt, and its more black-box semi-stochastic [37, 38], selected-CI-driven [39], and adaptive [40] descendants. The latter approach, which, along with $\text{CC}(t;3)$, is of interest in this work, allows one to converge high-level CC/EOMCC energetics using a recursively defined sequence of $\text{CC}(P;Q)$ calculations guided by the intrinsic structure of the $\text{CC}(P;Q)$ moment expansions without any reference to active orbitals or non-CC concepts. Although the $\text{CC}(P;Q)$ theory provides a general framework for describing ground as well as excited electronic states, so far only the semi-stochastic variant of it has been tested on excited-state energetics [37]. The present study helps to address this situation by applying the active-orbital-based $\text{CC}(t;3)$ and adaptive $\text{CC}(P;Q)$ approaches targeting CCSDT and EOMCCSDT to the ground- and excited-state PESs of water corresponding to the $\text{H}_2\text{O} \rightarrow \text{H} + \text{OH}$ dissociation.

2. Theory

Each $\text{CC}(P;Q)$ calculation requires defining two disjoint subspaces of the N -electron Hilbert space, referred to as the P space $\mathcal{H}^{(P)}$ and Q space $\mathcal{H}^{(Q)}$. The former space is spanned by the excited determinants $|\Phi_K\rangle = E_K|\Phi\rangle$, with E_K designating the elementary particle–hole excitation operator generating $|\Phi_K\rangle$ from the reference determinant $|\Phi\rangle$, which together with $|\Phi\rangle$ dominate the ground and excited electronic states of interest. The complementary subspace $\mathcal{H}^{(Q)}$ contains the excited determinants used to construct noniterative corrections to the energies obtained in the CC and EOMCC calculations in the P space, abbreviated as $\text{CC}(P)$ for the ground state and $\text{EOMCC}(P)$ for excited states.

In the $\text{CC}(P)$ computations, which are the first step of the $\text{CC}(P;Q)$ algorithm, we determine the cluster operator

$$T^{(P)} = \sum_{|\Phi_K\rangle \in \mathcal{H}^{(P)}} t_K E_K, \quad (1)$$

associated with the CC(P) ket state $|\Psi_0^{(P)}\rangle = e^{T^{(P)}}|\Phi\rangle$, and the corresponding ground-state energy $E_0^{(P)} = \langle\Phi|\bar{H}^{(P)}|\Phi\rangle$, where $\bar{H}^{(P)} = e^{-T^{(P)}}He^{T^{(P)}}$. In the subsequent EOMCC(P) step, we diagonalize the similarity-transformed Hamiltonian $\bar{H}^{(P)}$ in the P space to obtain the excited-state energies $E_\mu^{(P)}$ and the corresponding linear excitation operators

$$R_\mu^{(P)} = r_{\mu,0}\mathbf{1} + \sum_{|\Phi_K\rangle \in \mathcal{H}^{(P)}} r_{\mu,K}E_K \quad (2)$$

defining the EOMCC(P) ket states $|\Psi_\mu^{(P)}\rangle = R_\mu^{(P)}e^{T^{(P)}}|\Phi\rangle$. For both the ground ($\mu = 0$) and excited ($\mu > 0$) states, we also solve for the hole-particle deexcitation operators

$$L_\mu^{(P)} = \delta_{\mu,0}\mathbf{1} + \sum_{|\Phi_K\rangle \in \mathcal{H}^{(P)}} l_{\mu,K}(E_K)^\dagger, \quad (3)$$

which define the companion CC(P)/EOMCC(P) bra wave functions $\langle\tilde{\Psi}_\mu^{(P)}| = \langle\Phi|L_\mu^{(P)}e^{-T^{(P)}}$ satisfying the biorthonormality condition $\langle\tilde{\Psi}_\mu^{(P)}|\Psi_\nu^{(P)}\rangle = \delta_{\mu,\nu}$. Once the $T^{(P)}$, $R_\mu^{(P)}$, and $L_\mu^{(P)}$ operators and the CC(P) and EOMCC(P) energies $E_\mu^{(P)}$ are determined, we calculate the noniterative state-specific corrections

$$\delta_\mu(P; Q) = \sum_{|\Phi_K\rangle \in \mathcal{H}^{(Q)}} \ell_{\mu,K}(P) \mathfrak{M}_{\mu,K}(P), \quad (4)$$

where $\mathfrak{M}_{0,K}(P) = \langle\Phi_K|\bar{H}^{(P)}|\Phi\rangle$ and $\mathfrak{M}_{\mu,K}(P) = \langle\Phi_K|\bar{H}^{(P)}R_\mu^{(P)}|\Phi\rangle$ are the generalized moments of the CC(P) ($\mu = 0$) [30, 31] and EOMCC(P) ($\mu > 0$) [32] equations, which correspond to projections of these equations on the Q -space determinants $|\Phi_K\rangle \in \mathcal{H}^{(Q)}$, and the coefficients $\ell_{\mu,K}(P)$ multiplying moments $\mathfrak{M}_{\mu,K}(P)$ in Eq. (4) are defined as $\ell_{\mu,K}(P) = \langle\Phi|L_\mu^{(P)}\bar{H}^{(P)}|\Phi_K\rangle/D_{\mu,K}^{(P)}$, with $D_{\mu,K}^{(P)} = E_\mu^{(P)} - \langle\Phi_K|\bar{H}^{(P)}|\Phi_K\rangle$ representing the Epstein–Nesbet-like energy denominators. The final CC($P;Q$) energies are calculated as

$$E_\mu^{(P+Q)} = E_\mu^{(P)} + \delta_\mu(P; Q). \quad (5)$$

A key advantage of the CC($P;Q$) framework is the flexibility it offers in defining the P and Q spaces to accurately and efficiently capture the many-electron correlation effects relevant to the electronic states of interest. The present study exploits this freedom to examine the ground- and excited-state PESs of the water molecule along the O–H bond-breaking coordinate using three different types of the CC($P;Q$) methodology aimed at accurately approximating the high-level CCSDT/EOMCCSDT energetics. In the first CC($P;Q$) approach examined in this work, the P space is spanned by all singly and doubly excited determinants, $|\Phi_i^a\rangle$ and $|\Phi_{ij}^{ab}\rangle$, respectively, where i, j, \dots (a, b, \dots) denote the occupied (unoccupied) spinorbitals in $|\Phi\rangle$, and the Q space consists of all triply excited determinants $|\Phi_{ijk}^{abc}\rangle$. This conventional variant of CC($P;Q$) represents the noniterative triples corrections to the CCSD and EOMCCSD energies defining the ground-state CR-CC(2,3) method [26, 29, 33, 34, 41] and its excited-state CR-EOMCC(2,3) counterpart [26, 27, 29], which were used to determine the ground- and excited-state potentials of water in Ref. [13]. In the second CC($P;Q$) method, the P and Q spaces are constructed with the help of active orbitals such that the P space contains all singly and doubly excited determinants and the subset of triply excited determinants selected according to the formula $|\Phi_{i\mathbf{J}\mathbf{K}}^{Abc}\rangle$, where \mathbf{K} (\mathbf{A}) designate the occupied (unoccupied) spinorbitals around the Fermi level belonging to the user-specified active spinorbital set, and the Q space is spanned by the remaining triply excited determinants. This choice of P and Q spaces results in the CC(t;3) method of Refs. [29, 36], in which the ground-state CCSDt [44–47] and excited-state EOMCCSDt [11, 12, 47] energies are corrected for the remaining, largely dynamical, T_3 and $R_{\mu,3}$ correlation effects not captured by the CCSDt/EOMCCSDt calculations. In the third CC($P;Q$) variant considered in this study, the P space is spanned by all singly and doubly excited determinants and the leading triply excited determinants identified with the help of their $\ell_{\mu,K}(P) \mathfrak{M}_{\mu,K}(P)$ contributions to the $\delta_\mu(P; Q)$ corrections, Eq. (4), using the adaptive CC($P;Q$) algorithm introduced in Ref. [40], and the Q space consists of the remaining triply excited determinants not included in the P space. Each of the above CC($P;Q$) approaches aims at converging the CCSDT/EOMCCSDT energetics using the same general recipe defined by Eqs. (1) – (5). The only difference between them is in the method used to partition the manifold of triple excitations between the iterative and noniterative steps of the CC($P;Q$) calculations. All three

CC($P;Q$) approaches also offer major savings in the computational effort compared to the full treatment of triples, which were, for example, discussed, along with illustrative timings, in Refs. [40, 48] (cf. Ref. [37] for additional relevant remarks). It is, therefore, interesting to examine which of these three CC($P;Q$) schemes is most effective in capturing T_3 and $R_{\mu,3}$ correlations.

3. Results and Discussion

3.1. Computational Details

The nuclear geometries needed to construct the ground- and excited-state PESs of the water molecule along the $\text{H}_2\text{O} \rightarrow \text{H} + \text{OH}$ dissociation path, obtained by considering 11 values of the O–H bond separation R_{OH} ranging from 1.3 to 4.4 bohr, with the remaining O–H bond length and H–O–H bond angle optimized using the CCSD/cc-pVTZ method, were taken from Ref. [16]. As pointed out in Refs. [13, 16], the resulting dissociation pathway on the ground-state PES has several desirable characteristics. For example, the equilibrium values of R_{OH} and H–O–H bond angle resulting from the CCSD/cc-pVTZ geometry optimization, of 1.809 bohr and 103.9 degree, respectively, are in good agreement with experiment and, as R_{OH} increases, the second O–H bond length approaches its equilibrium value in the ground-state OH radical and the angular potential flattens. For each water structure corresponding to a particular value of R_{OH} , we carried out the CR-CC(2,3)/CR-EOMCC(2,3), active-orbital-based CC($P;Q$) [i.e., CC(t;3)], adaptive CC($P;Q$), and parent CCSDT/EOMCCSDT calculations for the four lowest $A'(C_s)$ -symmetric singlet states, which include the ground state X^1A' and n^1A' excited states with $n = 1-3$, three lowest $A'(C_s)$ -symmetric triplet states (denoted as n^3A' , $n = 1-3$), two lowest $A''(C_s)$ -symmetric singlet states (denoted as n^1A'' , $n = 1, 2$), and three lowest triplet states of the $A''(C_s)$ symmetry (denoted as n^3A'' , $n = 1-3$). To enable comparisons of our CCSDT/EOMCCSDT data with the full CI and MRCC energetics obtained in Refs. [16] (full CI and MRCC) and [13] (full CI), all calculations reported in this work were performed with the TZ basis set of Ref. [16], used in Ref. [13] as well. The restricted Hartree–Fock (RHF) determinant, used in our CC/EOMCC calculations as a reference, consisted of four $a'(C_s)$ -symmetric and one $a''(C_s)$ -symmetric orbitals. The lowest-energy orbital correlating with 1s shell of oxygen was frozen in post-RHF steps. To define the CC(t;3) and underlying CCSDt/EOMCCSDt calculations, the three highest occupied and two lowest unoccupied orbitals in the RHF reference correlating with 2p shell of oxygen and 1s shells of hydrogens were treated as active. Two of the three active occupied and both active unoccupied orbitals were of the $a'(C_s)$ symmetry. The third active occupied orbital was $a''(C_s)$ -symmetric. The adaptive CC($P;Q$) calculations employed the relaxed algorithm, discussed in detail in Ref. [40], in which we assumed a 1% growth rate in the numbers of triply excited determinants entering the underlying P spaces. The percentages of triply excited determinants characterizing our adaptive CC(P), EOMCC(P), and CC($P;Q$) calculations were defined as fractions of the $S_z = 0$ triples of the $A'(C_s)$ ($^1A'$ and $^3A'$ states) or $A''(C_s)$ ($^1A''$ and $^3A''$ states) symmetry identified with the adaptive CC($P;Q$) algorithm. The CCSD, EOMCCSD, CR-CC(2,3), CR-EOMCC(2,3), CCSDt, EOMCCSDt, CC(t;3), CCSDT, and EOMCCSDT computations were performed using our in-house CC/EOMCC codes interfaced with the RHF and integral transformation routines in GAMESS [49]. The adaptive CC($P;Q$) calculations were executed using our recently developed CCpy package available on GitHub [50] that can efficiently handle the potentially spotty subsets of triply excited determinants entering the underlying CC(P) and EOMCC(P) computations, which may not form continuous manifolds labelled by occupied and unoccupied orbitals from the respective ranges of indices, to achieve the desired speedups compared to CCSDT/EOMCCSDT (see Ref. [40] for further information).

The results of our CC/EOMCC calculations are shown in Tables 1 – 3, Fig. 1, and the Supplementary Data document (see Appendix A). Table 1 summarizes the mean unsigned error (MUE) and nonparallelity error (NPE) values characterizing the CCSDT and EOMCCSDT potential cuts of water computed in this work relative to their full CI counterparts obtained in Refs. [13, 16]. The MUE and NPE values characterizing the CCSD/EOMCCSD, CR-CC(2,3)/CR-EOMCC(2,3), adaptive CC(P)/EOMCC(P) and CC($P;Q$), CCSDt/EOMCCSDt, and CC(t;3) PESs relative to their CCSDT/EOMCCSDT parents are reported in Tables 2 and 3, respectively. The ground- and excited-state PES cuts of water corresponding to the $\text{H}_2\text{O} \rightarrow \text{H} + \text{OH}$ dissociation channels that correlate with the $X^2\Pi$ ground state and the lowest-energy $^2\Sigma^+$ and $^2\Sigma^-$ states of OH obtained with CCSD/EOMCCSD, CR-CC(2,3)/CR-EOMCC(2,3), adaptive CC(P)/EOMCC(P) and CC($P;Q$), CCSDt/EOMCCSDt, CC(t;3), and CCSDT/EOMCCSDT are shown in Fig. 1. The Supplementary Data document provides total electronic energies of all the calculated states.

3.2. Accuracy of the CCSDT and EOMCCSDT Approaches

Given that all three variants of the $CC(P;Q)$ methodology tested in this work aim at converging or accurately approximating the CCSDT/EOMCCSDT energetics, it is important to assess how well the CCSDT and EOMCCSDT approaches perform in describing the ground- and excited-state PESs of water along the O–H bond-breaking coordinate relative to their exact, full CI, counterparts. As shown in Table 1, the CCSDT method provides a highly accurate description of the X^1A' state, with the MUE and NPE values relative to the ground-state full CI potential being as small as 0.63 and 1.14 millihartree, respectively. EOMCCSDT is similarly accurate in describing the excited-state potentials, with only three – out of 11 examined in this study – characterized by the MUE and NPE values exceeding 1 and 3 millihartree, respectively, but even in this case, which includes the $2^1A'$, $3^1A'$, and $3^3A'$ states, the MUE and NPE values, of 1.28 and 3.19 millihartree for the $2^1A'$ PES, 1.53 and 4.48 millihartree for the $3^1A'$ PES, and 1.41 and 5.50 millihartree for the $3^3A'$ PES, remain rather small, especially when we realize that these three states are located hundreds of millihartrees above the ground state (cf. Supplementary Data). Most importantly, the EOMCCSDT approach accurately approximates the full CI water potentials in the highly stretched $R_{OH} \geq 2.4$ bohr region, where all excited states of interest in this study acquire a substantial MR character that EOMCCSD cannot capture. When compared with the MRCC results reported in Ref. [16], we observe that the SR CCSDT and EOMCCSDT methods can also rival, or even outperform, the state-of-the-art MR treatments. For example, for the $1^3A'$, $1^1A''$, $2^3A''$, $2^1A''$, $3^1A'$, and $3^3A'$ states, the EOMCCSDT NPE values relative to full CI are lower – sometimes substantially – than those resulting from the nR -GMS-SU-CCSD and (N, M) -CCSD calculations. For the X^1A' , $1^1A''$, $1^3A''$, $2^3A'$, and $2^1A'$ potentials, the CCSDT and EOMCCSDT NPE values relative to full CI are within ~ 1 millihartree from the best MRCC results reported in Ref. [16]. It is clear from these comparisons that we can treat the ground- and excited-state potentials of water along the O–H bond-breaking coordinate obtained with CCSDT and EOMCCSDT as highly accurate benchmarks for evaluating performance of the different $CC(P;Q)$ approaches explored in this work.

3.3. Performance of Different $CC(P;Q)$ Approaches Relative to CCSDT and EOMCCSDT

We begin by discussing the first variant of the $CC(P;Q)$ methodology of interest in the present study corresponding to the CR-CC(2,3) and CR-EOMCC(2,3) triples corrections to CCSD and EOMCCSD (also examined in Ref. [13]). In the vicinity of the equilibrium geometry on the ground-state PES, all $CC/EOMCC$ approaches, including CR-CC(2,3)/CR-EOMCC(2,3), and even CCSD/EOMCCSD, perform well. Indeed, the errors relative to CCSDT in the X^1A' potential computed with CCSD in the $R_{OH} = 1.3$ – 2.0 bohr region range between 2.771 and 3.562 millihartree. CR-CC(2,3) reduces them to ~ 0.2 – 0.3 millihartree. For the excited-state potentials in the $R_{OH} = 1.3$ – 2.0 bohr region, the largest error obtained with EOMCCSD relative to EOMCCSDT, which occurs when the high-lying $3^1A'$ state is considered, is 3.392 millihartree. The largest error characterizing CR-EOMCC(2,3) in the same region, encountered when the $3^3A''$ PES is examined, is 1.660 millihartree. For nearly all excited states considered in this work, the differences between the CR-EOMCC(2,3) and EOMCCSDT potentials in the $R_{OH} = 1.3$ – 2.0 bohr region are about 1 millihartree, making them virtually identical around the equilibrium geometry. The CR-EOMCC(2,3) PESs are also more parallel to their EOMCCSDT counterparts than the corresponding EOMCCSD surfaces.

The situation changes when we move toward larger R_{OH} values, where all electronic states of water considered in this study develop a strong MR character, resulting in failures of the CCSD and EOMCCSD methods, especially when the X^1A' , $1^1A''$, $1^3A''$, $1^1A'$, $2^3A'$, $2^3A''$, $2^1A'$, $3^3A''$, $3^1A'$, and $3^3A'$ potentials are examined. These failures become particularly dramatic for the $2^3A''$, $2^1A'$, $3^3A''$, and $3^1A'$ states, where errors relative to EOMCCSDT resulting from the EOMCCSD calculations in the $R_{OH} = 2.8$ – 4.4 bohr region become as large as 28.470, 32.540, 65.442, and 32.035 millihartree, respectively, although no state considered in our computations is accurately described when T_3 and $R_{\mu,3}$ correlations are neglected and $R_{OH} > 2.4$ bohr. The CR-CC(2,3) and CR-EOMCC(2,3) triples corrections reduce the excessive errors characterizing the X^1A' , $1^1A''$, $1^3A''$, $1^1A'$, $2^3A'$, $2^3A''$, $2^1A'$, $3^3A''$, $3^1A'$, and $3^3A'$ potentials obtained with CCSD/EOMCCSD at larger values of R_{OH} and the associated MUEs and NPEs shown in Tables 2 and 3, which are 6.154–28.262 and 8.453–64.663 millihartree, respectively, in the CCSD/EOMCCSD case and 0.543–6.075 and 0.692–42.170 millihartree when the CR-CC(2,3)/CR-EOMCC(2,3) data are examined, but several problems remain, especially when dealing with the $2^3A''$ and $3^3A''$ states. In the former case, the CR-EOMCC(2,3) approach produces large, 11.891–13.976 millihartree, errors relative to EOMCCSDT in the $R_{OH} = 4.0$ – 4.4 bohr region, resulting in the qualitatively incorrect asymptotic behavior of the CR-EOMCC(2,3) $2^3A''$ potential and the NPE of 13.043 millihartree. The CR-EOMCC(2,3) PES for the $3^3A''$ state presents an even more distressing situation, with a massive,

37.018 millihartree, error relative to EOMCCSDT at $R_{\text{OH}} = 2.8$ bohr associated with a bump in the $3^3\text{A}''$ potential seen in Fig. 1(b) and the even larger NPE value of 42.170 millihartree. These failures of CR-EOMCC(2,3) are consistent with our earlier observations [29, 36–40] that none of the triples corrections to CCSD/EOMCCSD can provide accurate results when T_3 and $R_{\mu,3}$ correlations become substantial and strongly coupled to their lower-rank counterparts, as is the case when examining the $2^3\text{A}''$ and $3^3\text{A}''$ potentials at larger R_{OH} values.

The above challenges encountered in the CR-EOMCC(2,3) calculations can be addressed by turning to the CC(t;3) method. As explained in Sec. 2, CC(t;3) is a CC(P ; Q) approach in which energies obtained in the CCSDt/EOMCCSDt calculations that incorporate the leading triply excited determinants identified with the help of active orbitals in the P spaces used in the iterative CC(P)/EOMCC(P) steps are corrected for the missing, mostly dynamical, T_3 and $R_{\mu,3}$ correlations using Eq. (4). The numerical results in Tables 2 and 3, with further details provided by Tables S2–S13 in Supplementary Data, and the potential curves shown in Fig. 1(h) demonstrate that the CC(t;3) method readily addresses the shortcomings of the CR-EOMCC(2,3) approach and its ground-state CR-CC(2,3) counterpart. This becomes particularly clear when examining the $2^3\text{A}''$ and $3^3\text{A}''$ potentials that are poorly described by CR-EOMCC(2,3). For example, the CC(t;3) calculations reduce the large, 11.891–13.976 millihartree, errors relative to EOMCCSDT obtained with CR-EOMCC(2,3) for the $2^3\text{A}''$ PES in the $R_{\text{OH}} = 4.0$ –4.4 bohr region to 0.481–0.625 millihartree. The massive error of 37.018 millihartree produced by CR-EOMCC(2,3) for the $3^3\text{A}''$ state at $R_{\text{OH}} = 2.8$ bohr is reduced in the CC(t;3) calculations by more than two orders of magnitude, to 0.133 millihartree, eliminating the unphysical bump in the CR-EOMCC(2,3) potential for this state in the $R_{\text{OH}} = 2.4$ –3.2 bohr region altogether. The major improvements offered by CC(t;3) in describing the $2^3\text{A}''$ and $3^3\text{A}''$ PESs are also reflected in the corresponding NPE values relative to EOMCCSDT, which decrease from 13.043 and 42.170 millihartree obtained with CR-EOMCC(2,3) to the minuscule 0.255 and 0.608 millihartree, respectively. In general, the CC(P ; Q)-based CC(t;3) method provides a highly accurate description of the ground and excited states of water along the O–H bond-breaking coordinate, greatly improving the CR-CC(2,3)/CR-EOMCC(2,3) energetics and closely matching the nearly exact CCSDt/EOMCCSDt potentials at small fractions of the computational costs associated with CCSDT/EOMCCSDT. This is manifested by the tiny MUE and NPE values relative to CCSDt/EOMCCSDT characterizing the CC(t;3) calculations for the 12 electronic states of water reported in this work, which range from 0.166 to 0.951 millihartree for MUEs and 0.110 to 0.608 millihartree for NPEs (see Tables 2 and 3). By capturing the missing T_3 and $R_{\mu,3}$ correlations, the CC(t;3) corrections are also very effective in improving the underlying CCSDt/EOMCCSDt potentials, especially in reducing the MUE values relative to CCSDt/EOMCCSDT characterizing the CCSDt and EOMCCSDt calculations, from 1.477–2.420 millihartree in CCSDt/EOMCCSDt to fractions of a millihartree in CC(t;3).

We conclude by commenting on the results of our adaptive CC(P ; Q) calculations, which are based on the same basic principles as those employed in the CC(t;3) considerations, but do not rely on active orbitals to obtain accurate results, allowing us to converge the high-level CCSDT and EOMCCSDT energetics in an entirely black-box fashion. As shown in Tables 2 and 3, panels (d) and (f) of Fig. 1, and Tables S2–S13 in Supplementary Data, the adaptive CC(P ; Q) approach is remarkably effective in accurately approximating the CCSDt/EOMCCSDT water potentials. Already with a tiny 1% of triply excited determinants in the underlying P spaces, the adaptive CC(P ; Q) calculations offer major improvements in the CR-CC(2,3)/CR-EOMCC(2,3) data. They reduce the MUE and NPE values of 0.543 and 0.692 millihartree, respectively, relative to CCSDT, obtained with CR-CC(2,3) for the ground-state potential, to less than 0.3 millihartree. The improvements in the description of the 11 excited states of water considered in this work offered by the adaptive CC(P ; Q) approach using the leading 1% of triply excited determinants in the underlying P spaces, which for the sake of brevity of this discussion will be abbreviated as CC(P ; Q)[%T = 1], are similarly impressive, especially when we realize that in the case of the C_s -symmetric water structures and the TZ basis set used in our calculations, 1% of triply excited determinants amounts to only about 300 T_3 and $R_{\mu,3}$ amplitudes, as opposed to 31,832 $A'(C_s)$ -symmetric and 32,232 $A''(C_s)$ -symmetric $S_z = 0$ triples used by full CCSDT/EOMCCSDT. These improvements can be best seen when comparing the $2^3\text{A}''$ and $3^3\text{A}''$ potentials obtained with CR-EOMCC(2,3) with their CC(P ; Q)[%T = 1] counterparts. In the case of the $2^3\text{A}''$ PES, the MUE and NPE values of 5.033 and 13.043 millihartree relative to EOMCCSDT resulting from the CR-EOMCC(2,3) computations are reduced to 1.177 and 1.081 millihartree, respectively, when the CC(P ; Q)[%T = 1] approach is employed, helping to alleviate the inaccurate behavior of CR-EOMCC(2,3) in the asymptotic part of the $2^3\text{A}''$ potential. The poor description of the $3^3\text{A}''$ PES by the CR-EOMCC(2,3) method becomes much more reasonable in the CC(P ; Q)[%T = 1] calculations as well. The 37.018 millihartree error relative to EOMCCSDT obtained with CR-EOMCC(2,3) at $R_{\text{OH}} = 2.8$ bohr reduces to 6.740 millihartree when the adaptive CC(P ; Q)[%T = 1] approach is employed. The MUE and NPE values

characterizing the CR-EOMCC(2,3) $3^3A''$ potential, of 6.075 and 42.170 millihartree, respectively, decrease in the $CC(P;Q)[\%T = 1]$ calculations to 1.949 and 5.933 millihartree and, as shown in Fig. 1 (d), the unphysical bump in the CR-EOMCC(2,3) PES for this state in the $R_{OH} = 2.4\text{--}3.2$ bohr region disappears. The generally small MUE and NPE values characterizing the $CC(P;Q)[\%T = 1]$ calculations for the 12 PESs of water considered in this study, relative to their CCSDT/EOMCCSDT parents, which range from 0.275 to 1.949 millihartree for MUEs and 0.216 to 5.933 millihartree for NPEs, are certainly encouraging. As shown in Tables 2 and 3, Fig. 1(f), and Tables S2–S13 in Supplementary Data, the situation gets even better when the fraction of triply excited determinants included in the P spaces defining the adaptive $CC(P;Q)$ calculations increases to 2%. The MUEs and NPEs relative to CCSDT/EOMCCSDT characterizing the resulting $CC(P;Q)[\%T = 2]$ computations for the 12 potential cuts of water examined in this work reduce to 0.197–0.993 and 0.133–1.572 millihartree, respectively. In the case of the $2^3A''$ and $3^3A''$ potentials that cause major troubles to the CR-EOMCC(2,3) method, the already small MUEs obtained in the $CC(P;Q)[\%T = 1]$ calculations, of 1.177 and 1.949 millihartree, decrease to 0.737 and 0.993 millihartree, respectively, when the fraction of triply excited determinants incorporated in the underlying P spaces grows from 1% to 2%. The corresponding NPE values decrease from 1.081 and 5.933 millihartree in the $CC(P;Q)[\%T = 1]$ case to 0.237 and 1.572 millihartree, when the $CC(P;Q)[\%T = 2]$ approach is employed. For some electronic potentials of water, the NPEs characterizing the adaptive $CC(P;Q)[\%T = 2]$ computations are slightly larger than those obtained with the $CC(t;3)$ approach, but the overall performance of the adaptive $CC(P;Q)[\%T = 2]$ and $CC(t;3)$ methods is very similar. This is promising for the future applications of the adaptive $CC(P;Q)$ framework since typical $CC(t;3)$ computations, in addition to requiring the user to select active orbitals, employ considerably larger fractions of triply excited determinants in the iterative steps of the underlying $CC(P;Q)$ algorithm than their black-box adaptive $CC(P;Q)$ counterparts. For example, the $CC(t;3)$ calculations reported in this work used about 38% of all triples in the iterative CCSDt/EOMCCSDt steps, as opposed to only 2% used in the adaptive $CC(P;Q)$ computations producing virtually identical results.

4. Summary

We extended the active-orbital-based and adaptive $CC(P;Q)$ methodologies of Refs. [29, 36, 40] to excited electronic states and used the resulting approaches aimed at converging the CCSDT and EOMCCSDT energetics to determine the ground- and excited-state potentials of the water molecule along the O–H bond-breaking coordinate, for which CCSDT and EOMCCSDT accurately approximate the full CI data. We demonstrated that the active-orbital-based $CC(P;Q)$ method, abbreviated as $CC(t;3)$, and its black-box adaptive $CC(P;Q)$ counterpart are similarly effective in accurately approximating the parent CCSDT/EOMCCSDT energetics at small fractions of the computational costs, improving the results obtained with the CR-CC(2,3) and CR-EOMCC(2,3) triples corrections to CCSD/EOMCCSD, but the adaptive $CC(P;Q)$ approach produced potentials of the CCSDT/EOMCCSDT quality with much smaller fractions of triply excited determinants in the underlying P spaces than those used by $CC(t;3)$. In our future work, we will investigate if the excellent performance of the active-orbital-based and adaptive $CC(P;Q)$ methods demonstrated in this study holds for other molecular systems and larger basis sets, for which full CI and CCSDT/EOMCCSDT calculations, used in this work to assess accuracies of the various $CC(P;Q)$ approaches, are no longer possible.

CRedit authorship contribution statement

Karthik Gururangan: Methodology, Software, Data curation, Formal analysis, Validation, Writing - original draft. **Jun Shen:** Methodology, Software, Data curation, Formal analysis, Validation, Writing - original draft. **Piotr Piecuch:** Conceptualization, Methodology, Formal analysis, Investigation, Funding acquisition, Project administration, Resources, Supervision, Validation, Writing - reviewing and editing.

Declaration of competing interest

The authors declare that they have no known competing financial interests or personal relationships that could have appeared to influence the work reported in this paper.

Data availability

The data that support the findings of this study are available within the article and the Supplementary Data.

Acknowledgments

This work has been supported by the Chemical Sciences, Geosciences and Biosciences Division, Office of Basic Energy Sciences, Office of Science, U.S. Department of Energy (Grant No. DE-FG02-01ER15228 to P.P.).

Appendix A. Supplementary data

Supplementary data to this article can be found online at

References

- [1] J. Čížek, On the correlation problem in atomic and molecular systems. Calculation of wavefunction components in Ursell-type expansion using quantum-field theoretical methods, *J. Chem. Phys.* 45 (1966) 4256–4266. doi:10.1063/1.1727484.
- [2] J. Čížek, On the use of the cluster expansion and the technique of diagrams in calculations of correlation effects in atoms and molecules, *Adv. Chem. Phys.* 14 (1969) 35–89. doi:10.1002/9780470143599.ch2.
- [3] J. Paldus, J. Čížek, I. Shavitt, Correlation problems in atomic and molecular systems. IV. Extended coupled-pair many-electron theory and its application to the BH_3 molecule, *Phys. Rev. A* 5 (1972) 50–67. doi:10.1103/PhysRevA.5.50.
- [4] K. Emrich, An extension of the coupled cluster formalism to excited states (I), *Nucl. Phys. A* 351 (1981) 379–396. doi:10.1016/0375-9474(81)90179-2.
- [5] J. F. Stanton, R. J. Bartlett, The equation of motion coupled-cluster method. A systematic biorthogonal approach to molecular excitation energies, transition probabilities, and excited state properties, *J. Chem. Phys.* 98 (1993) 7029–7039. doi:10.1063/1.464746.
- [6] H. J. Monkhorst, Calculation of properties with the coupled-cluster method, *Int. J. Quant. Chem., Symp.* 11 (1977) 421–432. doi:10.1002/qua.560120850.
- [7] D. Mukherjee, P. K. Mukherjee, A response-function approach to the direct calculation of the transition-energy in a multiple-cluster expansion formalism, *Chem. Phys.* 39 (1979) 325–335. doi:10.1016/0301-0104(79)80153-6.
- [8] H. Koch, P. Jørgensen, Coupled cluster response functions, *J. Chem. Phys.* 93 (1990) 3333–3344. doi:10.1063/1.458814.
- [9] H. Koch, H. J. A. Jensen, P. Jørgensen, T. Helgaker, Excitation energies from the coupled cluster singles and doubles linear response function (CCSDLR). Applications to Be , CH^+ , CO , and H_2O , *J. Chem. Phys.* 93 (1990) 3345–3350. doi:10.1063/1.458815.
- [10] H. Nakatsuji, Cluster expansion of the wavefunction. Excited states, *Chem. Phys. Lett.* 59 (1978) 362–364. doi:10.1016/0009-2614(78)89113-1.
- [11] K. Kowalski, P. Piecuch, The active-space equation-of-motion coupled-cluster methods for excited electronic states: Full EOMCCSDt, *J. Chem. Phys.* 115 (2001) 643–651. doi:10.1063/1.1378323.
- [12] K. Kowalski, P. Piecuch, Excited-state potential energy curves of CH^+ : A comparison of the EOMCCSDt and full EOMCCSDT results, *Chem. Phys. Lett.* 347 (2001) 237–246. doi:10.1016/S0009-2614(01)01010-7.
- [13] J. J. Lutz, P. Piecuch, Performance of the completely renormalized equation-of-motion coupled-cluster method in calculations of excited-state potential cuts of water, *Comput. Theor. Chem.* 1040–1041 (2014) 20–34. doi:10.1016/j.comptc.2014.05.008.
- [14] P. Piecuch, J. A. Hansen, A. O. Ajala, Benchmarking the completely renormalised equation-of-motion coupled-cluster approaches for vertical excitation energies, *Mol. Phys.* 113 (2015) 3085–3127. doi:10.1080/00268976.2015.1076901.
- [15] S. A. Kucharski, M. Włoch, M. Musiał, R. J. Bartlett, Coupled-cluster theory for excited electronic states: The full equation-of-motion coupled-cluster single, double, and triple excitation method, *J. Chem. Phys.* 115 (2001) 8263–8266. doi:10.1063/1.1416173.
- [16] X. Li, J. Paldus, Performance of multireference and equation-of-motion coupled-cluster methods for potential energy surfaces of low-lying excited states: Symmetric and asymmetric dissociation of water, *J. Chem. Phys.* 133 (2010) 024102. doi:10.1063/1.3451074.
- [17] J. Noga, R. J. Bartlett, The full CCSDT model for molecular electronic structure, *J. Chem. Phys.* 86 (1987) 7041–7050, 89 (1988) 3401 [Erratum]. doi:10.1063/1.452353.
- [18] G. E. Scuseria, H. F. Schaefer, III, A new implementation of the full CCSDT model for molecular electronic structure, *Chem. Phys. Lett.* 152 (1988) 382–386. doi:10.1016/0009-2614(88)80110-6.
- [19] J. D. Watts, R. J. Bartlett, Economical triple excitation equation-of-motion coupled-cluster methods for excitation energies, *Chem. Phys. Lett.* 233 (1995) 81–87. doi:10.1016/0009-2614(94)01434-W.
- [20] O. Christiansen, H. Koch, P. Jørgensen, Perturbative triple excitation corrections to coupled cluster singles and doubles excitation energies, *J. Chem. Phys.* 105 (1996) 1451–1459. doi:10.1063/1.472007.
- [21] J. D. Watts, R. J. Bartlett, Iterative and non-iterative triple excitation corrections in coupled-cluster methods for excited electronic states: The EOM-CCSDT-3 and EOM-CCSD(\bar{T}) methods, *Chem. Phys. Lett.* 258 (1996) 581–588. doi:10.1016/0009-2614(96)00708-7.
- [22] O. Christiansen, H. Koch, P. Jørgensen, Response functions in the CC3 iterative triple excitation model, *J. Chem. Phys.* 103 (1995) 7429–7441. doi:10.1063/1.470315.
- [23] S. Hirata, M. Nooijen, I. Grabowski, R. J. Bartlett, Perturbative corrections to coupled-cluster and equation-of-motion coupled-cluster energies: A determinantal analysis, *J. Chem. Phys.* 114 (2001) 3919–3928, 115 (2001) 3967–3968 [Erratum]. doi:10.1063/1.1346578.

- [24] T. Shiozaki, K. Hirao, S. Hirata, Second- and third-order triples and quadruples corrections to coupled-cluster singles and doubles in the ground and excited states, *J. Chem. Phys.* 126 (2007) 244106. doi:10.1063/1.2741262.
- [25] K. Kowalski, P. Piecuch, New coupled-cluster methods with singles, doubles, and noniterative triples for high accuracy calculations of excited electronic states, *J. Chem. Phys.* 120 (2004) 1715–1738. doi:10.1063/1.1632474.
- [26] M. Włoch, M. D. Lodriguito, P. Piecuch, J. R. Gour, Two new classes of non-iterative coupled-cluster methods derived from the method of moments of coupled-cluster equations, *Mol. Phys.* 104 (2006) 2149–2172, 104 (2006) 2991 [Erratum]. doi:10.1080/00268970600659586.
- [27] P. Piecuch, J. R. Gour, M. Włoch, Left-eigenstate completely renormalized equation-of-motion coupled-cluster methods: Review of key concepts, extension to excited states of open-shell systems, and comparison with electron-attached and ionized approaches, *Int. J. Quantum Chem.* 109 (2009) 3268–3304. doi:10.1002/qua.22367.
- [28] G. Fradelos, J. J. Lutz, T. A. Wesolowski, P. Piecuch, M. Włoch, Embedding vs supermolecular strategies in evaluating the hydrogen-bonding-induced shifts of excitation energies, *J. Chem. Theory Comput.* 7 (2011) 1647–1666. doi:10.1021/ct200101x.
- [29] J. Shen, P. Piecuch, Biorthogonal moment expansions in coupled-cluster theory: Review of key concepts and merging the renormalized and active-space coupled-cluster methods, *Chem. Phys.* 401 (2012) 180–202. doi:10.1016/j.chemphys.2011.11.033.
- [30] P. Piecuch, K. Kowalski, In search of the relationship between multiple solutions characterizing coupled-cluster theories, in: J. Leszczyński (Ed.), *Computational Chemistry: Reviews of Current Trends*, Vol. 5, World Scientific, Singapore, 2000, pp. 1–104. doi:10.1142/9789812792501_0001.
- [31] K. Kowalski, P. Piecuch, The method of moments of coupled-cluster equations and the renormalized CCSD[T], CCSD(T), CCSD(TQ), and CCSDT(Q) approaches, *J. Chem. Phys.* 113 (2000) 18–35. doi:10.1063/1.481769.
- [32] K. Kowalski, P. Piecuch, New type of noniterative energy corrections for excited electronic states: Extension of the method of moments of coupled-cluster equations to the equation-of-motion coupled-cluster formalism, *J. Chem. Phys.* 115 (2001) 2966–2978. doi:10.1063/1.1386794.
- [33] P. Piecuch, M. Włoch, Renormalized coupled-cluster methods exploiting left eigenstates of the similarity-transformed Hamiltonian, *J. Chem. Phys.* 123 (2005) 224105. doi:10.1063/1.2137318.
- [34] P. Piecuch, M. Włoch, J. R. Gour, A. Kinal, Single-reference, size-extensive, non-iterative coupled-cluster approaches to bond breaking and biradicals, *Chem. Phys. Lett.* 418 (2006) 467–474. doi:10.1016/j.cpllett.2005.10.116.
- [35] P. Piecuch, J. A. Hansen, D. Staedter, S. Faure, V. Blanchet, Communication: Existence of the doubly excited state that mediates the photoionization of azulene, *J. Chem. Phys.* 138 (2013) 201102. doi:10.1063/1.4808014.
- [36] J. Shen, P. Piecuch, Combining active-space coupled-cluster methods with moment energy corrections via the CC(*P*; *Q*) methodology, with benchmark calculations for biradical transition states, *J. Chem. Phys.* 136 (2012) 144104. doi:10.1063/1.3700802.
- [37] S. H. Yuwono, A. Chakraborty, J. E. Deustua, J. Shen, P. Piecuch, Accelerating convergence of equation-of-motion coupled-cluster computations using the semi-stochastic CC(*P*; *Q*) formalism, *Mol. Phys.* 118 (2020) e1817592. doi:10.1080/00268976.2020.1817592.
- [38] J. E. Deustua, J. Shen, P. Piecuch, Converging high-level coupled-cluster energetics by Monte Carlo sampling and moment expansions, *Phys. Rev. Lett.* 119 (2017) 223003. doi:10.1103/PhysRevLett.119.223003.
- [39] K. Gururangan, J. E. Deustua, J. Shen, P. Piecuch, High-level coupled-cluster energetics by merging moment expansions with selected configuration interaction, *J. Chem. Phys.* 155 (2021) 174114. doi:10.1063/5.0064400.
- [40] K. Gururangan, P. Piecuch, Converging high-level coupled-cluster energetics via adaptive selection of excitation manifolds driven by moment expansions, *J. Chem. Phys.* 159 (2023) 084108. doi:10.1063/5.0162873.
- [41] M. Włoch, J. R. Gour, P. Piecuch, Extension of the renormalized coupled-cluster methods exploiting left eigenstates of the similarity-transformed Hamiltonian to open-shell systems: A benchmark study, *J. Phys. Chem. A* 111 (2007) 11359–11382. doi:10.1021/jp0725351.
- [42] N. Oliphant, L. Adamowicz, Coupled-cluster method truncated at quadruples, *J. Chem. Phys.* 95 (1991) 6645–6651. doi:10.1063/1.461534.
- [43] S. A. Kucharski, R. J. Bartlett, The coupled-cluster single, double, triple, and quadruple excitation method, *J. Chem. Phys.* 97 (1992) 4282–4288. doi:10.1063/1.463930.
- [44] N. Oliphant, L. Adamowicz, The implementation of the multireference coupled-cluster method based on the single-reference formalism, *J. Chem. Phys.* 96 (1992) 3739–3744. doi:10.1063/1.461878.
- [45] P. Piecuch, N. Oliphant, L. Adamowicz, A state-selective multireference coupled-cluster theory employing the single-reference formalism, *J. Chem. Phys.* 99 (1993) 1875–1900. doi:10.1063/1.466179.
- [46] P. Piecuch, S. A. Kucharski, R. J. Bartlett, Coupled-cluster methods with internal and semi-internal triply and quadruply excited clusters: CCSDt and CCSDtq approaches, *J. Chem. Phys.* 110 (1999) 6103–6122. doi:10.1063/1.478517.
- [47] P. Piecuch, Active-space coupled-cluster methods, *Mol. Phys.* 108 (2010) 2987–3015. doi:10.1080/00268976.2010.522608.
- [48] I. Magoulas, N. P. Bauman, J. Shen, P. Piecuch, Application of the CC(*P*; *Q*) hierarchy of coupled-cluster methods to the beryllium dimer, *J. Phys. Chem. A* 122 (2018) 1350–1368. doi:10.1021/acs.jpca.7b10892.
- [49] G. M. J. Barca, C. Bertoni, L. Carrington, D. Datta, N. De Silva, J. E. Deustua, D. G. Fedorov, J. R. Gour, A. O. Gunina, E. Guidez, T. Harville, S. Irle, J. Ivanic, K. Kowalski, S. S. Leang, H. Li, W. Li, J. J. Lutz, I. Magoulas, J. Mato, V. Mironov, H. Nakata, B. Q. Pham, P. Piecuch, D. Poole, S. R. Pruitt, A. P. Rendell, L. B. Roskop, K. Ruedenberg, T. Sattasathuchana, M. W. Schmidt, J. Shen, L. Slipchenko, M. Sosonkina, V. Sundriyal, A. Tiwari, J. L. G. Vallejo, B. Westheimer, M. Włoch, P. Xu, F. Zahariev, M. S. Gordon, Recent developments in the general atomic and molecular electronic structure system, *J. Chem. Phys.* 152 (2020) 154102. doi:10.1063/5.0005188.
- [50] K. Gururangan and P. Piecuch, “CCpy: A Coupled-Cluster Package Written in Python,” see <https://github.com/piecuch-group/ccpy> [software].

Table 1

The MUE and NPE values, in millihartree, relative to full CI characterizing the ground-state CCSDT and excited-state EOMCCSDT potentials of the water molecule, as described by the TZ basis set of Ref. [16], along the O–H bond-breaking coordinate corresponding to the $\text{H}_2\text{O} \rightarrow \text{H} + \text{OH}$ dissociation.

	X^1A'	$1^1A''$	$1^3A'$	$1^3A''$	$1^1A'$	$2^3A'$	$2^3A''$	$2^1A'$	$2^1A''$	$3^3A''$	$3^1A'$	$3^3A'$
MUE	0.63	0.78	0.28	0.90	0.92	0.93	0.43	1.28	0.59	0.63	1.53	1.41
NPE	1.14	1.85	0.83	2.14	2.13	2.33	1.35	3.19	0.57	2.67	4.48	5.50

Table 2

The MUE values, in millihartree, relative to CCSDT/EOMCCSDT characterizing the ground- and excited-state potential cuts of the water molecule, as described by the TZ basis set of Ref. [16], along the O–H bond-breaking coordinate corresponding to the $\text{H}_2\text{O} \rightarrow \text{H} + \text{OH}$ dissociation obtained with the different $\text{CC}(P)/\text{EOMCC}(P)$ and $\text{CC}(P;Q)$ approaches examined in the present work.

State	CCSD ^a	CR(2,3) ^b	CCSDt ^c	CC(t;3) ^d	%T = 1 ^e		%T = 2 ^f	
					CC(<i>P</i>)	CC(<i>P</i> ;Q)	CC(<i>P</i>)	CC(<i>P</i> ;Q)
X^1A'	6.154	0.543	2.047	0.166	2.176	0.275	1.616	0.197
$1^1A''$	7.666	1.517	1.683	0.599	3.159	0.755	2.271	0.622
$1^3A'$	2.819	1.137	1.741	0.951	2.061	0.793	1.532	0.616
$1^3A''$	7.693	1.080	1.658	0.627	3.237	0.854	2.339	0.665
$1^1A'$	10.103	1.544	1.602	0.589	3.578	0.590	2.420	0.494
$2^3A'$	8.846	1.225	1.682	0.646	3.379	0.665	2.322	0.530
$2^3A''$	9.258	5.033	1.565	0.590	5.384	1.177	3.532	0.737
$2^1A'$	14.460	2.988	2.276	0.718	3.230	0.782	2.359	0.618
$2^1A''$	2.337	1.750	1.477	0.553	3.461	0.870	2.535	0.579
$3^3A''$	28.262	6.075	2.420	0.542	8.111	1.949	4.973	0.993
$3^1A'$	13.547	2.410	1.688	0.804	5.151	1.152	3.120	0.643
$3^3A'$	8.305	2.481	1.656	0.854	3.794	1.048	2.671	0.676

^a CCSD for the ground state and EOMCCSD for excited states.

^b CR-CC(2,3) for the ground state and CR-EOMCC(2,3) for excited states.

^c CCSDt/EOMCCSDt calculations using the active space consisting of the three highest occupied and two lowest unoccupied RHF orbitals.

^d CC(t;3) calculations using the active space consisting of the three highest occupied and two lowest unoccupied RHF orbitals.

^e $\text{CC}(P)/\text{EOMCC}(P)$ and $\text{CC}(P;Q)$ calculations using *P* spaces consisting of all singly and doubly excited determinants and 1% of triply excited determinants identified by the adaptive $\text{CC}(P;Q)$ algorithm.

^f $\text{CC}(P)/\text{EOMCC}(P)$ and $\text{CC}(P;Q)$ calculations using *P* spaces consisting of all singly and doubly excited determinants and 2% of triply excited determinants identified by the adaptive $\text{CC}(P;Q)$ algorithm.

Table 3

The NPE values, in millihartree, relative to CCSDT/EOMCCSDT characterizing the ground- and excited-state potential cuts of the water molecule, as described by the TZ basis set of Ref. [16], along the O–H bond-breaking coordinate corresponding to the $\text{H}_2\text{O} \rightarrow \text{H} + \text{OH}$ dissociation obtained with the different $\text{CC}(P)/\text{EOMCC}(P)$ and $\text{CC}(P;Q)$ approaches examined in the present work.

State	CCSD ^a	CR(2,3) ^b	CCSDt ^c	CC(t;3) ^d	%T = 1 ^e		%T = 2 ^f	
					CC(<i>P</i>)	CC(<i>P</i> ; <i>Q</i>)	CC(<i>P</i>)	CC(<i>P</i> ; <i>Q</i>)
X^1A'	8.453	0.692	0.687	0.110	1.072	0.216	0.801	0.159
$1^1A''$	16.093	4.592	0.446	0.275	1.569	0.433	1.304	0.198
$1^3A'$	5.004	0.442	0.452	0.492	0.801	0.593	1.005	0.281
$1^3A''$	17.445	3.303	0.447	0.240	2.070	0.430	1.360	0.133
$1^1A'$	21.043	4.637	0.387	0.244	2.692	0.313	1.380	0.168
$2^3A'$	20.127	3.712	0.826	0.257	2.264	0.246	1.233	0.218
$2^3A''$	29.017	13.043	0.572	0.255	6.852	1.081	2.761	0.237
$2^1A'$	33.260	8.330	2.231	0.271	2.216	0.761	1.434	0.508
$2^1A''$	7.971	3.983	0.601	0.263	3.129	0.611	0.837	0.636
$3^3A''$	64.663	42.170	3.601	0.608	23.376	5.933	10.679	1.572
$3^1A'$	30.846	4.757	0.463	0.603	6.019	2.207	2.862	0.993
$3^3A'$	21.562	5.670	0.712	0.392	3.149	1.574	1.413	0.582

^a CCSD for the ground state and EOMCCSD for excited states.

^b CR-CC(2,3) for the ground state and CR-EOMCC(2,3) for excited states.

^c CCSDt/EOMCCSDt calculations using the active space consisting of the three highest occupied and two lowest unoccupied RHF orbitals.

^d CC(t;3) calculations using the active space consisting of the three highest occupied and two lowest unoccupied RHF orbitals.

^e $\text{CC}(P)/\text{EOMCC}(P)$ and $\text{CC}(P;Q)$ calculations using *P* spaces consisting of all singly and doubly excited determinants and 1% of triply excited determinants identified by the adaptive $\text{CC}(P;Q)$ algorithm.

^f $\text{CC}(P)/\text{EOMCC}(P)$ and $\text{CC}(P;Q)$ calculations using *P* spaces consisting of all singly and doubly excited determinants and 2% of triply excited determinants identified by the adaptive $\text{CC}(P;Q)$ algorithm.

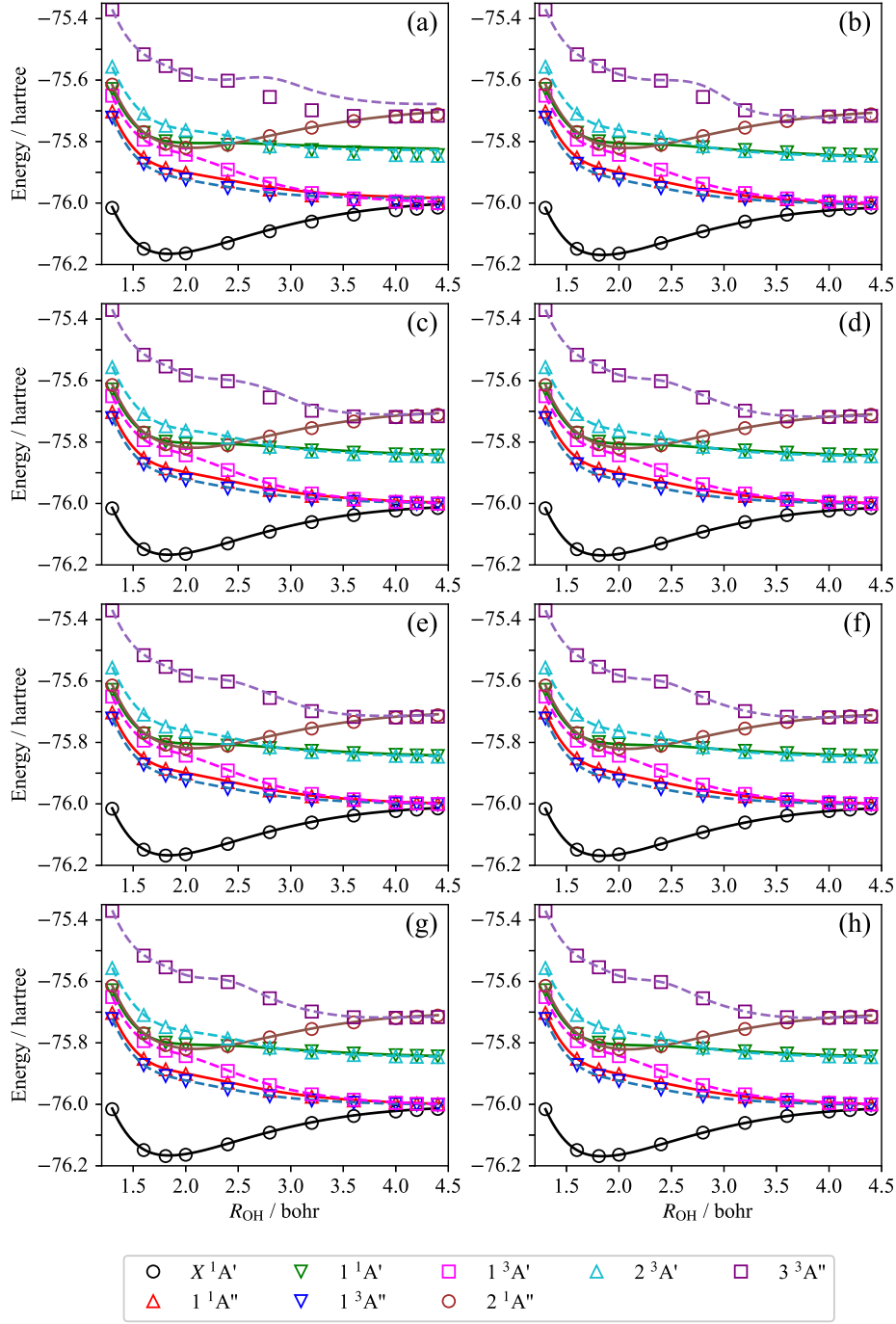


Fig. 1. A comparison of the potential cuts of water, plotted as functions of R_{OH} and corresponding to the $H_2O \rightarrow H + OH$ dissociation channels that correlate with the $X^2\Pi$ ground state and the lowest-energy $^2\Sigma^+$ and $^2\Sigma^-$ states of OH, obtained with (a) CCSD/EOMCCSD, (b) CR-CC(2,3)/CR-EOMCC(2,3), (c) adaptive CC(P)/EOMCC(P) using 1% of triply excited determinants in the P spaces, (d) adaptive CC(P;Q) using 1% of triply excited determinants in the P spaces, (e) adaptive CC(P)/EOMCC(P) using 2% of triply excited determinants in the P spaces, (f) adaptive CC(P;Q) using 2% of triply excited determinants in the P spaces, (g) CCSDt/EOMCCSDt, and (h) CC(t;3) with their full CCSDT/EOMCCSDT counterparts. The splined CCSD/EOMCCSD, CR-CC(2,3)/CR-EOMCC(2,3), adaptive CC(P)/EOMCC(P), adaptive CC(P;Q), CCSDt/EOMCCSDt, and CC(t;3) data are represented by the solid and dashed lines, whereas the open circles, squares, triangles, and inverted triangles correspond to the parent CCSDT/EOMCCSDT energetics.